

Metal-enhanced fluorescence from zinc substrates can lead to spectral distortion and a wavelength dependence

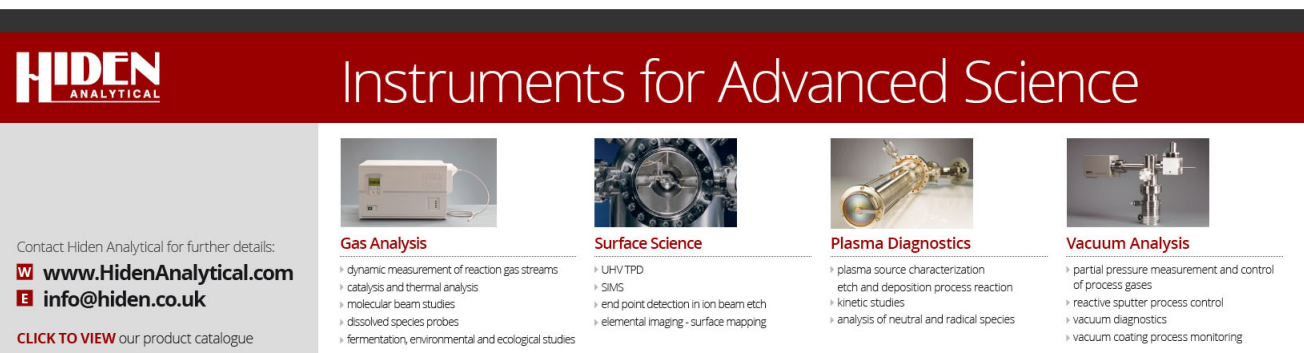
Hilla Ben Hamo, Jan Karolin, Buddha Mali, Ariel Kushmaro, Robert Marks, and Chris D. Geddes

Citation: [Applied Physics Letters](#) **106**, 081605 (2015); doi: 10.1063/1.4913671

View online: <http://dx.doi.org/10.1063/1.4913671>

View Table of Contents: <http://scitation.aip.org/content/aip/journal/apl/106/8?ver=pdfcov>

Published by the [AIP Publishing](#)

The advertisement for Hiden Analytical features a dark red header with the company logo and the slogan 'Instruments for Advanced Science'. Below the header, four columns of text describe different instrument categories: Gas Analysis, Surface Science, Plasma Diagnostics, and Vacuum Analysis. Each category includes a list of specific applications and services. The Gas Analysis section lists dynamic measurement of reaction gas streams, catalysis and thermal analysis, molecular beam studies, dissolved species probes, and fermentation, environmental and ecological studies. The Surface Science section lists UHV TPD, SIMS, end point detection in ion beam etch, and elemental imaging - surface mapping. The Plasma Diagnostics section lists plasma source characterization, etch and deposition process reaction, kinetic studies, and analysis of neutral and radical species. The Vacuum Analysis section lists partial pressure measurement and control of process gases, reactive sputter process control, vacuum diagnostics, and vacuum coating process monitoring. Contact information for Hiden Analytical is provided on the left side of the advertisement.

HIDEN
ANALYTICAL

Instruments for Advanced Science

Contact Hiden Analytical for further details:
W www.HidenAnalytical.com
E info@hiden.co.uk
CLICK TO VIEW our product catalogue

Gas Analysis

- › dynamic measurement of reaction gas streams
- › catalysis and thermal analysis
- › molecular beam studies
- › dissolved species probes
- › fermentation, environmental and ecological studies

Surface Science

- › UHV TPD
- › SIMS
- › end point detection in ion beam etch
- › elemental imaging - surface mapping

Plasma Diagnostics

- › plasma source characterization
- › etch and deposition process reaction
- › kinetic studies
- › analysis of neutral and radical species

Vacuum Analysis

- › partial pressure measurement and control of process gases
- › reactive sputter process control
- › vacuum diagnostics
- › vacuum coating process monitoring

Metal-enhanced fluorescence from zinc substrates can lead to spectral distortion and a wavelength dependence

Hilla Ben Hamo,^{1,2} Jan Karolin,² Buddha Mali,² Ariel Kushmaro,¹ Robert Marks,¹ and Chris D. Geddes^{2,a)}

¹Department of Biotechnology Engineering, Faculty of Engineering Science, Ben-Gurion University of the Negev, P.O. Box 653, Beer-Sheva 84105, Israel

²Department of Chemistry and BioChemistry, Institute of Fluorescence, University of Maryland Baltimore County, The Columbus Center, 701 East Pratt St., Baltimore 21202, USA

(Received 9 January 2015; accepted 15 February 2015; published online 25 February 2015)

Metal-enhanced fluorescence enhancement factors up to 7-fold have been observed for Basic Fuchsin (BF) in close proximity to Zinc nano particulate substrates. In addition, the emission spectra of BF close-to Zinc as compared to a control sample are heavily distorted, particularly on the red-edge, giving systematic trends in enhancement, anywhere from 3- to 7-fold. We discuss these remarkable wavelength dependent effects with regard to the mechanism of metal-enhanced fluorescence. © 2015 AIP Publishing LLC. [<http://dx.doi.org/10.1063/1.4913671>]

In the last 15 years, there has been a significant literature on metal-enhanced fluorescence (MEF),¹⁻⁴ where the near-field interactions of plasmon supporting nanoparticles with fluorophores typically give rise to spectroscopically favorable properties, such as enhanced fluorescence and a much improved system photostability. Most of the reports of MEF have focused on silver, due to its visible wavelength plasmon band and the subsequent ability to enhance fluorescence in the visible spectral region. Other metals have also been used to plasmon-enhance fluorescence, including gold,⁵ copper,⁶ Aluminum,⁷ and Zinc.⁸ Gold and copper nanoparticles typically enhance fluorescence in the red to near-IR region, while Aluminum and Zinc have particular advantages in the UV and visible spectral regions. Since the report of MEF from Zinc substrates by Geddes *et al.*,⁸ there have been numerous other reports.^{9,10} However, in all these reports for Zinc and indeed, all of the metals, there has been virtually no reports of spectral distortions of fluorophores. Karolin and Geddes¹¹ recently demonstrated *experimentally* spectral shifts from copper substrates with Rhodamine 800 in the red spectral region (> 700 nm), but there have been no reports in the UV or visible region to date. In addition, Le Ru has theoretically predicted spectral distortions,^{12,13} although the fast-coupling and coupling from non-vibronically relaxed states would ultimately lead to blue-shifted emission spectra, which has not been experimentally observed to date either. Subsequently, in this letter, we show that similar to copper,¹¹ metal-enhanced fluorescence from Zinc substrates also leads to significant spectral distortion on the red edge of the spectra, with systematic changes in the enhancement factor observed, *in essence*, a wavelength dependence in enhancement. However, in contrast to the recent work on copper, the spectra observed from Zinc show an increased full-width-at-half maxima (FWHM), i.e., the spectra are broader.

Basic Fuchsin and 99.995% pure Zinc were purchased from Sigma-Aldrich, USA and Kurt J. Lesker Company,

Material Group, Clariton, PA, USA, respectively. Fisher brand glass slides were first washed with double dionized water and ethanol (histological grade, Fisher Scientific, USA), dried, and then plasma cleaned for 10 min. An Edwards 360 thermal vapor deposition system was used for the Zinc deposition at a rate of 0.3 nm/s, under a typically pressure of 5×10^{-6} torr. A quartz crystal oscillator was used to monitor the rate and the film thickness. A Cary 60 Bio UV-Vis spectrometer (Agilent) was used to record the absorbance spectra. Standard $4 \times 1 \times 1$ cm cuvettes were used for Basic Fuchsin aqueous solutions, the Zinc slides were oriented perpendicular to the beam. The absorbance spectra were recorded relative to a background signal sample, uncoated glass and a cuvette filled with water, respectively.

Synchronous scattering spectra, i.e., spectra recorded when the emission wavelength = excitation wavelength ($\lambda_{\text{Ex}} = \lambda_{\text{Em}}$), were obtained on a Cary Eclipse, Varian, Inc., equipped with a plate reader. To minimize background signal, samples were placed on absorptive neutral density filters before being mounted perpendicular to the beam in the plate reader. Basic Fuchsin emission spectra were recorded using a Fluoromax 4P, Horiba, NJ, USA, in a standard $4 \times 1 \times 1$ cm cuvette. Emission spectra of Basic Fuchsin from Zinc films of different thicknesses were recorded on a HR 2000 spectrograph from Ocean Optics. The samples were excited parallel to the surface using a 405 nm laser, Power Technology Inc, AR, USA. The excitation power was adjusted using a variable neutral density filter and the power subsequently recorded on a PM100D power meter (model S121C from Thor labs). The emission was collected through a 600 μm core diameter optic fiber from Ocean Optics, passing through a 510 nm long pass filter (Edmund Optics), removing unwanted scattered excitation light.

Zinc nanoparticulate films were deposited on glass slides, and showed a broad plasmon band, <500 nm, Figure 1(a), consistent with a previous report.⁸ The unpolarized synchronous scattering spectra, i.e., when the excitation wavelength equals the emission wavelength, are shown in 1B. The synchronous scattering spectra are a convolution of both

^{a)}Author to whom correspondence should be addressed. Electronic mail: Chrisgeddes74@gmail.com

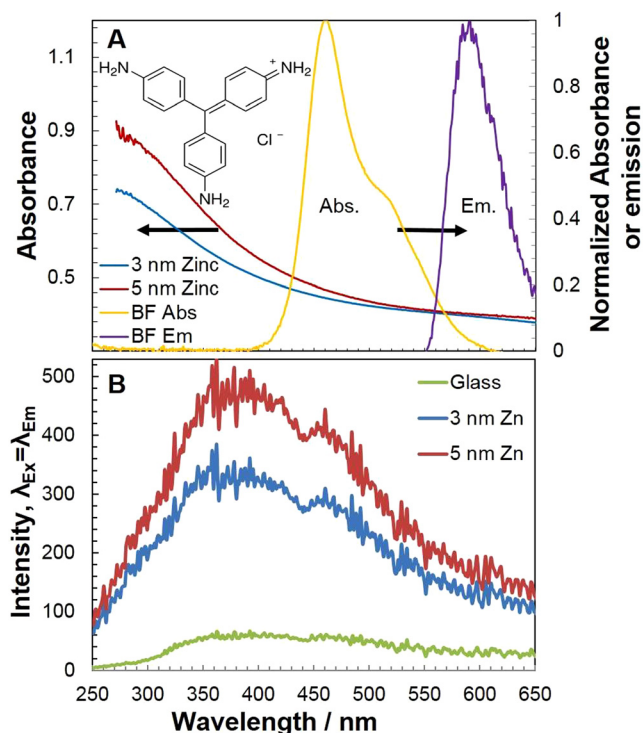


FIG. 1. (A) BF aqueous solution absorbance and emission spectra. Absorbance of different Zinc thicknesses (3, 5 nm). (B) Synchronous scattering spectra ($\lambda_{Ex} = \lambda_{Em}$) from both a glass slide (control sample) and Zinc coated slides (samples).

the absorption and scattering properties of the surface, and have been shown previously to be a good indicator of both the magnitude and wavelength dependence of MEF.¹⁴ Given that large nanoparticles are dominated by the scattering portion of the extinction spectrum, i.e., scales as $r^{6,15}$ we can clearly see the synchronous spectra centered ≈ 380 , i.e., red-shifted, as compared to the absorption spectra of the Zinc films in Figure 1(a). As expected, a 5 nm Zinc film scatters more intensely and is red-shifted as compared to a 3 nm thick Zinc nanoparticulate film.

Figure 2(a) shows the emission spectra of Basic Fuchsin (BF) from both a 3 nm thick Zinc film and from a glass slide, a control sample which does not contain plasmon enhancing metal. Dividing these spectra, we readily generate the MEF spectra, dotted line of Figure 2(a). These MEF spectra show a wavelength dependence and have not *hitherto* been reported for Zinc. Interestingly, the MEF spectra appear to peak with a mean enhancement value ≈ 6 . It is important to note that for nearly all the reports of MEF in the literature, these MEF spectra are flat, i.e., there is no wavelength dependence of enhancement observed. When the spectra are normalized, Figure 2(b), we observe a broader metal-enhanced fluorescence BF spectrum, as compared to the control sample. This is in contrast to a previous report from copper substrates, where the greatest enhancements were accompanied by spectra with more reduced FWHM. We also studied the effects of different solvents on the position of the emission spectrum and can conclude that the spectral shifts observed here are not due to a polarity effect on the fluorophore. Similar trends and results were observed for the 5 nm thick Zinc nanoparticulate films, Figures 3(a) and 3(b).

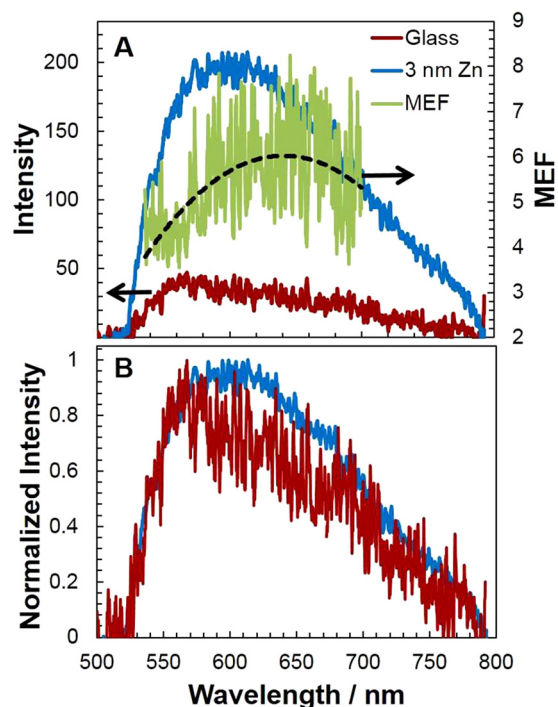


FIG. 2. (A) Emission spectra recorded for BF aqueous solution on glass (control sample) and glass coated with a 3 nm Zn film (sample). The calculated MEF response is also shown, i.e., the emission response from the sample divided by the control sample, with the mean value shown, dotted line. (B) Normalized spectra from both glass and zinc.

Figure 4(a) shows the emission spectra from glass and the 1,2,3,5, and 10 nm thick Zinc films studied. As the thickness of the Zinc film increases, the enhancement factor (emission from Zinc divided by the emission from the glass control

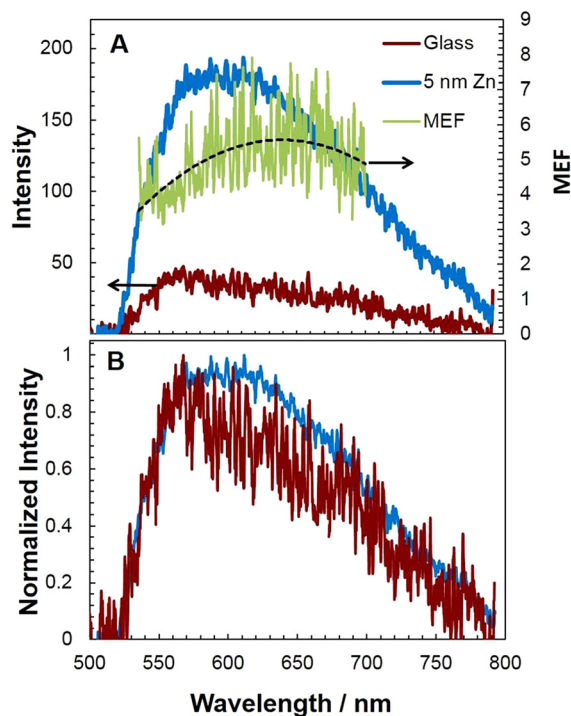


FIG. 3. (A) Emission spectra recorded for BF aqueous solution on glass (control sample) and glass coated with a 5 nm Zn film (sample). The calculated wavelength dependence of MEF is also shown, with the mean value shown, dotted line. (B) Normalized emission spectra from both glass and zinc.

sample) increases to a maximum enhancement for 3 nm Zinc and then slightly decreases for both 5 and then 10 nm thicknesses, Figure 4(b). The FWHM remains roughly constant, except for the 3 nm thickness, i.e., the largest enhancement, which was significantly reduced, not like what was observed in a previous paper pertaining to spectral distortions from copper films.¹¹ At first, one may think that this result is simply experimental error. However, the spectra presented here are the mean spectra from 3 positions over the Zinc surface, the results and trends being reproducible. Subsequently, similar to the previous copper report,¹¹ the film which provides the greatest enhancement in intensity also shows a narrower emission spectra, i.e., a reduced FWHM.

Finally, it is important to place our findings in context with the broader and current MEF thinking today. The only theoretical work to address spectral profile modifications in MEF has been undertaken by Le Ru *et al.*,^{12,13} some time back, with little experimental work being undertaken to date. Le Ru suggests that there are three possibilities for relaxation in a coupled MEF system, slow, fast, and ultrafast electron relaxation. For the slow MEF case, the excited electron relaxes to $S_1(0)$ from which it can then decay to S_0 . We consider this to be the standard MEF condition, similar to classical far-field fluorescence. For the fast relaxation condition, decay to the ground state, S_0 , may occur from any intermediate levels of S_1 after absorption and the lowest level, $S_1(0)$. In Le Ru's ultra fast MEF model, the fluorophore radiative decay rate in the presence of metal is assumed to be much faster, where no electron relaxation occurs in S_1 , the emission being from $S_1(n)$ to $S_0(n)$, where n is the n th vibronic level. In both the fast and ultra fast decay models, the

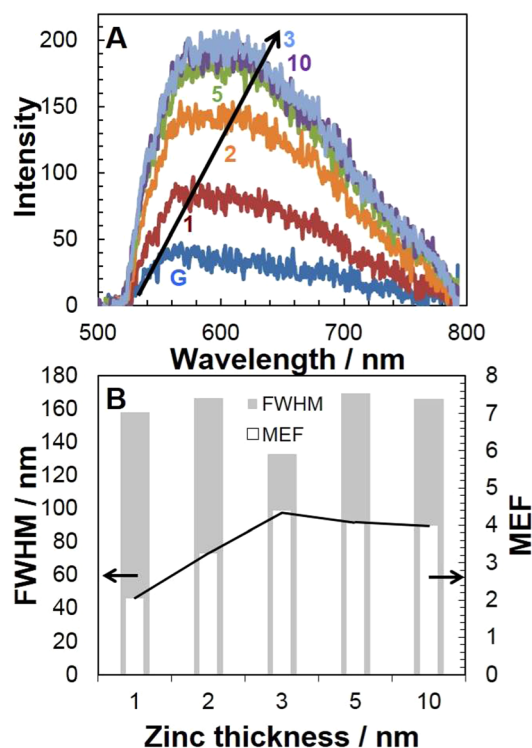


FIG. 4. (A) Emission Spectra recorded for BF aqueous solution on glass (control sample) and glass coated with different thicknesses of Zinc (1, 2, 3, 5, and 10 nm). (B) The calculated MEF magnitude and the FWHM of each Zinc thickness. G—glass control slide.

assumption is made that the fluorophore is both excited and that the fluorophore emits the coupled quanta itself, i.e., the metal is simply modifying the radiative decay rate of the fluorophore. Interestingly, if the fluorophore were indeed radiating/decaying faster when in close proximity to metal, then one would typically expect to see a blue shifted spectrum as compared to the control sample, which is decaying in the free space condition. This is because in classical fluorescence, the observed steady-state fluorescence spectrum is a solvent relaxed spectra. If a fluorophore is subsequently decaying quicker near-to metal, it follows that the solvent will not have had time to fully relax, and hence, a blue shifted spectrum would be expected. This effect was originally predicted by Geddes and Lakowicz in 2002 [Fig. 10 in Ref. 16], the theory being developed by Le Ru *et al.* in 2007,¹² but has not been experimentally verified.

Interestingly, the experimental data to date from both copper substrates and the Zinc data presented here clearly indicate a red shifted and red-edge distorted spectrum, which is not in agreement with the earlier predictions of both Geddes and Lakowicz¹⁶ and Le Ru *et al.*¹² One possible explanation to this discrepancy is that in both predictions, MEF has been attributed to a metal-modified *fluorophore* radiative decay rate. In recent years, Geddes has postulated a different mechanism for MEF, whereby the excited fluorophore non-radiatively transfers energy to the surface plasmons, the nanoparticle itself subsequently radiating the coupled quanta. We therefore speculate whether the different plasmon energy levels, thought to be a continuum of possible states, of the nanoparticle account for the spectral distortions observed. Work is currently under way in our laboratory to understand the origins of spectral distortions in MEF with regard to the radiating plasmon model (RPM) postulated by Geddes.¹⁷

In conclusion, we have observed spectral distortion for a fluorophore when located in the near-field close-to Zinc nanoparticulate films. This spectral distortion occurs on the red-edge of the emission spectrum and accounts for the wavelength dependence of MEF. The results for Zinc are not like those observed previously for copper films and do not appear to support the spectral profile modifications originally predicted by Geddes and Lakowicz in 2002 and theoretically by Le Ru *et al.* in 2007, predictions underpinned by models employing fluorophore radiative rate modifications.

¹C. D. Geddes, *Phys. Chem. Chem. Phys.* **15**(45), 19537 (2013).

²N. Sui, L. Wang, T. Yan, F. Liu, J. Sui, Y. Jiang, J. Wan, M. Liu, and W. Yu, *Sens. Actuators B* **202**, 1148–1153 (2014).

³M. Bauch, K. Toma, M. Toma, Q. Zhang, and J. Dostalek, *Plasmonics* **9**(4), 781–799 (2014).

⁴M. Ganguly, C. Mondal, J. Chowdhury, J. Pal, A. Pal, and T. Pal, *Dalton Trans.* **43**(3), 1032–1047 (2014).

⁵L. Zhang, Y. Song, T. Fujita, Y. Zhang, M. Chen, and T.-H. Wang, *Adv. Mater.* **26**(8), 1289–1294 (2014).

⁶Y. Zhang, K. Aslan, M. J. R. Previte, and C. D. Geddes, *Appl. Phys. Lett.* **90**(17), 173116 (2007).

⁷M. H. Chowdhury, K. Ray, S. K. Gray, J. Pond, and J. R. Lakowicz, *Anal. Chem.* **81**(4), 1397–1403 (2009).

⁸K. Aslan, M. J. R. Previte, Y. Zhang, and C. D. Geddes, *J. Phys. Chem. C* **112**(47), 18368–18375 (2008).

⁹R. Matsumoto, H. Yonemura, and S. Yamada, *J. Phys. Chem. C* **117**(6), 2486–2493 (2013).

¹⁰X. Zhang, L. Fu, J. Liu, Y. Kuang, L. Luo, D. G. Evans, and X. Sun, *Chem. Commun.* **49**(34), 3513–3515 (2013).

¹¹J. Karolin and C. Geddes, *Appl. Phys. Lett.* **105**(6), 063102 (2014).

- ¹²E. C. Le Ru, P. G. Etchegoin, J. Grand, N. Félidj, J. Aubard, and G. Lévi, *J. Phys. Chem. C* **111**(44), 16076–16079 (2007).
- ¹³E. C. L. Ru, J. Grand, N. Félidj, J. Aubard, G. Lévi, A. Hohenau, J. R. Krenn, E. Blackie, and P. G. Etchegoin, in *Metal-Enhanced Fluorescence*, edited by C. D. Geddes (John Wiley & Sons, Inc., 2010), pp. 25–65.
- ¹⁴A. I. Dragan, B. Mali, and C. D. Geddes, *Chem. Phys. Lett.* **556**, 168–172 (2013).
- ¹⁵K. Aslan, I. Gryczynski, J. Malicka, E. Matveeva, J. R. Lakowicz, and C. D. Geddes, *Curr. Opin. Biotechnol.* **16**(1), 55–62 (2005).
- ¹⁶C. Geddes and J. Lakowicz, *J. Fluorescence* **12**(2), 121–129 (2002).
- ¹⁷K. Aslan, Z. Leonenko, J. Lakowicz, and C. Geddes, *J. Fluorescence* **15**(5), 643–654 (2005).